IEEE Access
Multidisciplinary ⋮ Rapid Review ⋮ Open Access Journal

Received 16 May 2023, accepted 28 May 2023, date of publication 1 June 2023, date of current version 12 June 2023.

Digital Object Identifier 10.1109/ACCESS.2023.3282163

RESEARCH ARTICLE

Wavefront Control of Millimeter Waves With a VO_2-Based Reconfigurable Meta-Reflectarray

MOHAMMAD ALI SHAMELI[1], ANTONIO-D CAPOBIANCO[1,3], (Member, IEEE), LUCA SCHENATO[1,3], (Member, IEEE), MARCO SANTAGIUSTINA[1,3], (Member, IEEE), AND DOMENICO DE CEGLIA[2,3,4], (Member, IEEE)

[1]Department of Information Engineering, University of Padua, 35131 Padua, Italy
[2]Department of Information Engineering, University of Brescia, 25123 Brescia, Italy
[3]National Inter-University Consortium for Telecommunications (CNIT), 43124 Parma, Italy
[4]National Institute of Optics, National Research Council, 25123 Brescia, Italy

Corresponding author: Mohammad Ali Shameli (Mohammadali.shameli@unipd.it)

This work was partially supported by the European Union under the Italian National Recovery and Resilience Plan (NRRP) of NextGenerationEU, partnership on "Telecommunications of the Future" (PE0000001 - program "RESearch and innovation on future Telecommunications systems and networks, to make Italy more smART (RESTART)"), by University of Padova (SEED-BIRD2020) and by the Ministero dell'Istruzione, dell'Università e della Ricerca [Italian Ministry for Education, Universities and Research (MIUR)] (PRIN 2017HP5KH7_003 - FIRST).

ABSTRACT In this paper, a novel architecture of a reconfigurable metasurface is proposed and numerically assessed for wavefront control in wireless systems working in the millimeter-wave range. We show that a metasurface made of engineered silicon bricks covered with a thin film of vanadium dioxide provides anomalous reflection with an efficiency of 93% at 60 GHz and a relative bandwidth of 15%. After applying a thermal stimulus that triggers the transition of vanadium dioxide from the insulator phase to the metallic phase, the metasurface abruptly changes its response and provides specular reflection. The device shows high efficiency and broadband operation in both VO_2 states, allowing dynamic control of millimeter waves. Therefore, it finds applications in imaging, sensing, and intelligent wireless communications in 5G and 6G systems, especially for beam-shaping and beam-steering. Moreover, the proposed reconfigurable metasurface has a simple configuration that lends itself to standard fabrication tools, and it has a subwavelength size for integrated and compact communication systems.

INDEX TERMS Millimeter waves, reconfigurable structures, reflective metasurface, controlling phase front, phase-transition materials.

I. INTRODUCTION

Millimeter waves with a spectrum between 30 GHz and 300 GHz have proven to be one of the most promising and attractive bands for wireless communication [1], [2], [3]. Most wireless consumers with microwave frequencies below 6 GHz have limited data rates. Thus, demanding a larger spectrum bandwidth with a higher data rate requires an increase in the carrier frequency from the microwave to the millimeter-wave range [1], [4], [5]. Millimeter waves also play an essential role in realizing fifth- (5G) and sixth-generation (6G) cellular systems. 5G and 6G provide enormous free spectrum, gigabit-per-second data rates, and very low latency using the millimeter band in cellular communication systems [4], [5], [6]. Other relevant applications of millimeter wave technology are in self-driving and autonomous cars, where the design of multiple-input-multiple-output (MIMO) antennas operating in this regime will provide high data rates for real-time connection to other cars [7], [8], [9].

The growth of millimeter wave communications requires the development of various devices that can radiate, receive, and control millimeter waves. In particular, reconfigurable structures with fast tuning of the electromagnetic response are essential for high data rates. In addition, intelligent wireless communication systems that can prevent unwanted diffraction and loss of millimeter waves require the design of smart devices that can direct power in the desired direction

The associate editor coordinating the review of this manuscript and approving it for publication was Bilal Khawaja.

while maintaining large directivity. There has been a growing interest in developing reconfigurable devices for millimeter waves in the last few years. In reference [10], a high-gain, frequency-reconfigurable metasurface antenna has been proposed in which vanadium dioxide (VO_2) allows to change the operational bandwidth. A reconfigurable metasurface working at 100 GHz was shown to be capable of tunable steering of electromagnetic waves [11]. A digital coding metasurface has been designed with a nematic liquid crystal to realize different reflection phases tuned by DC-bias voltage [12]. A reconfigurable dielectric resonator antenna with a 360° adjustable pattern was proposed in [13]. In that work, reconfigurability was obtained by symmetrically placing six electromagnetic bandgaps (EBG). Another reconfigurable structure has been reported in [14], which is based on a wideband millimeter-wave Fabry–Pérot cavity (FPC) antenna with switched-beam radiation at a frequency of 60 GHz [14]. Nevertheless, the reconfigurable devices proposed so far [10], [12], [13], [14] are antennas, and, in most cases, they are not capable of forming or deflecting a millimeter-wave beam; also, in reference [11], the deflection efficiency is limited to 50%.

In addition, in reference [15], a tunable thermal radiation metasurface using a graphene-metal hybrid structure has been designed for infrared anticounterfeiting and information encryption with applications in energy harvesting and thermal management. Other advanced graphene-based structures are proposed and experimentally investigated in reference [16] to detect hemoglobin biomolecules based on analysis of the transmittance of the structure. Another recently proposed device is an all-optical plasmonic flip-flop metasurface designed in the THz frequency range, which can be controlled by tuning the chemical potential of graphene [17]. Programmable manipulation of terahertz beams was proposed with a reflective hybrid graphene-metal coding configuration, combining C-shaped metallic split-ring resonators with graphene [18].

Reconfigurability of the electromagnetic response of metasurfaces may be achieved with different materials. One of the tuning mechanisms is provided by conductive oxides. For example, an active metasurface based on indium-tin-oxide (ITO) was proposed in [19]. Phase transition materials (PTM) are activated by applying an external DC-bias voltage or a temperature stimulus [20], [21], [22]. Changing the crystallographic phase of germanium antimony telluride (GST) leads to terahertz wave control and modulation capabilities on the picosecond time scale [23]. Another example based on liquid crystals is a flexible millimeter antenna array for 5G networks [24]. 4-*N*, *N*-dimethylamino-4'-*N*'-methyl-stilbazolium tosylate (DAST) [25] provides a method of tailoring directional light scattering from a low-loss metasurface. Although these approaches [20], [21], [22], [23], [24], [25] lead to some degree of reconfigurability, in some configurations they may show low operational speed in the millimeter-wave range [24], [26], limitations due to feasibility [25], and, in some cases, limited performances [20], [23]. To solve these significant challenges, we have selected VO_2 as PTM, which allows fast tuning and deep modulation depths, and undergoes an abrupt and reversible switch between an insulator state to a metallic one. Indeed, VO_2 has a reversible phase transition between a high-resistivity insulating state at room temperature and a low-resistivity metallic state at a critical temperature of 68 °C [10], [11], [27], [28]. Additionally, VO_2 is the most promising thermochromic material in terms of feasibility, stability, and commercialization due to its cost efficiency and performance, especially in the millimeter band [10], [11], [27], [28].

The most critical problem that has not been addressed by previous works [10], [11], [12], [13], [14] is designing a simple, yet effective, architecture of reconfigurable metasurface for millimeter waves. Here, we propose and numerically investigate a novel structure for reconfigurable wavefront engineering of millimeter waves based on a meta-reflectarray made of silicon resonators covered by a VO_2 thin film for applications in beam-shaping and beam-steering in intelligent wireless communication systems, high-resolution imaging, sensing and also MIMO antennas for controlling the direction of millimeter-wave propagation. Also, this structure can be employed as a thermally-controlled switch. The proposed design, thanks to the VO_2 phase transition, provides highly efficient anomalous reflection when VO_2 is in the insulating state. In contrast, it switches to a highly efficient specular reflector when VO_2 switches to the metallic state. The switching is achieved by inducing a change the VO_2 film temperature. Compared to previous works on VO_2-based reconfigurable devices working in the millimeter-wave range, the structure proposed here shows significant improvements: it proposes a novel and simple architecture to control reflection by tuning the temperature of the VO_2 layer, it can be easily fabricated thanks to its simple configuration, it shows high efficiency and broadband operation in both the VO_2 states.

II. PROPOSED STRUCTURE

The proposed structure is illustrated in Fig. 1. We designed a meta-reflectarray made of silicon resonators covered by a VO_2 film. The structure switches the angle of the reflected wave when the operating temperature increases above the critical temperature of the VO_2 phase transition (T_C = 68 °C). The substrate is made of copper (Cu), and the thickness of the VO_2 "skin" layer is 50 μm, larger than the penetration depth of the metallic state of VO_2 in the millimeter-wave range (30-300GHz), which is about 15 μm based on the resistivity data (2.6×10^{-5} - 5×10^{-4} Ω.m [30], [31]). When VO_2 is in the insulator state, it has a relative permittivity of 9. In this situation, Si and VO_2 have similar electromagnetic behavior [32], [33]. Therefore, the thin layer of VO_2 plays a marginal role in the interaction with incident waves since its thickness is much smaller than the wavelength in the medium ($\lambda \sim 0.5$ mm). In the insulator state of VO_2, at temperatures below T_C, the supercell of the metasurface, shown in Fig. 1(b), is designed to provide anomalous, off-normal reflection with an angle of 30° under plane-wave illumination at normal incidence. However, after

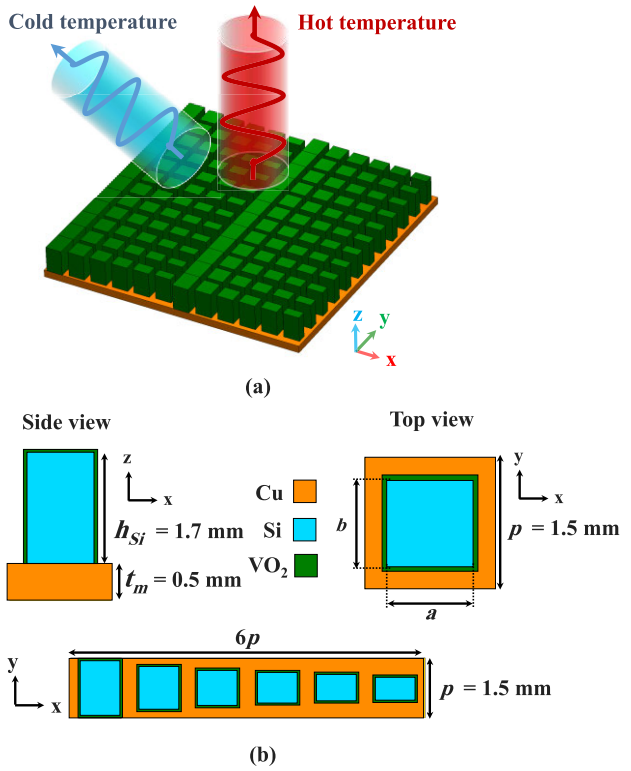

FIGURE 1. (a) Cross-sectional view from the side (xz-plane), and (b) cross-sectional view from the top (xy-plane) of the reconfigurable reflective metasurface with Si resonators with a thickness of $h_{Si} = 1.7$ mm covered by VO_2 skin layer with a thickness of 50μm. Also, the base unit cell size is $p = 1.5$ mm, and the lateral dimensions are a and b, in the direction of the x-axis and y-axis, respectively. The backplane is made of copper with a thickness of $t_m = 0.5$ mm.

the thermally-induced phase transition occurs, the VO_2 layer behaves as a metallic film that screens electromagnetic waves and prevents them from reaching the silicon metasurface underneath. In the metallic state of VO_2, the structure reflects all the incident waves in the specular (normal) direction.

III. BACKGROUND THEORY AND DESIGN

To realize beamforming at room temperature, the metasurface should provide a phase discontinuity $\phi(x)$, calculated by the generalized Snell's law [34], [35]:

$$\sin\theta_r - \sin\theta_i = \frac{1}{k_o}\frac{d\phi(x)}{dx}, \tag{1}$$

where θ_r and θ_i are the angles of reflected and incident waves, and k_0 is the free-space propagation constant of the plane wave. The electromagnetic wave impinges at an angle $\theta_i = 0°$, and the reflected wave should be in the desired anomalous direction. Thus, considering $k_0 = 2\pi/\lambda$ where λ is the wavelength in the vacuum, the phase profile of the reflected wave should be equal to:

$$\phi(x) = \frac{2\pi x}{\lambda} \times \sin\theta_r. \tag{2}$$

Eq (2) is the target phase profile that is required to deflect a normally-incident input plane wave at any arbitrary angle θ_r. To achieve the desired phase profile $\phi(x)$, one of the lateral dimensions of the Si bricks is fixed to $a = 1$ mm, and the other, b, is changed from 0.02 to 1.43 mm. Changing the lateral dimension of the silicon brick allows covering the phase of reflection between -180° and +180°, thus, any phase profile can be provided to deflect millimeter waves at any arbitrary angle. For illustrative purposes, we set the deflection angle $\theta_r = 30°$ so that the phase profile of the reflected wave should be equal to:

$$\phi(x) = \frac{\pi x}{\lambda}. \tag{3}$$

The desired phase profile in eq. (3) is achieved with the supercell reported in Fig. 1(b), after applying the design procedure detailed below. The procedure's main goal is to achieve maximum reflection amplitude (ideally 100%) and simultaneously obtain full control over the phase of the reflected wave [34], [36].

To characterize the behavior of silicon resonators with variable size, and in particular, to calculate the phase of the reflection coefficient as a function of the resonator shape and size, we perform full-wave simulations in the frequency domain with the commercial software CST Microwave Studio® using the finite-difference frequency-domain method (FDFD). The unit cell, containing one resonator with a specific shape and size, has lateral size equal to p along the x and y-axis, and periodic boundary conditions are set on the boundaries perpendicular to this axis. This is a standard choice in designing metasurfaces [37]. In the simulations, a plane wave is normally incident on the metasurface with an electric field polarized in the direction of the x-axis. Based on the experimental data in ref [32], there is a negligible variation in silicon relative permittivity at the millimeter wave frequency range, thus, we assumed a constant relative permittivity of 11.7. For VO_2, we consider a constant relative permittivity equal to 9 in the insulator state (below T_C), and for high temperature, we use the frequency-dependent Drude model, $\varepsilon = \varepsilon_\infty - \omega_p^2/(\omega^2 - j\omega\gamma)$, with $\varepsilon_\infty = 12$, plasma frequency $\omega_p = 1.4 \times 10^{15}$ rad/s, and collision frequency $\gamma = 5.75 \times 10^{13}$ 1/s in the metallic state [33], [38], [39], [40]. Also, the Drude model, fitted to the experimental data reported in [41], is adopted for the frequency-dependent permittivity of copper. The parameters used in the Drude model are $\varepsilon = \varepsilon_\infty - \omega_p^2/(\omega^2 - j\omega\gamma)$, with $\varepsilon_\infty = 4.68$, $\omega_p = 1.32 \times 10^{15}$ rad/s, and the collision frequency is $\gamma = 10.5 \times 10^{13}$ 1/s. To investigate the proposed device in both states of VO_2, we consider two different simulations at low temperature (below T_C) and high temperature (above T_C). The phase of the reflection coefficient is reported in the inset of Fig. 2 as a function of b, the lateral dimension of the silicon brick.

Using the data of the inset of Fig. 2, the size of the silicon bricks in the supercell (see Table. 1) has been chosen to provide the target phase profile of eq. (3), as reported in Fig. 2. The real phase profile, limited by the discretization effect of the metasurface, perfectly overlaps the target one leading

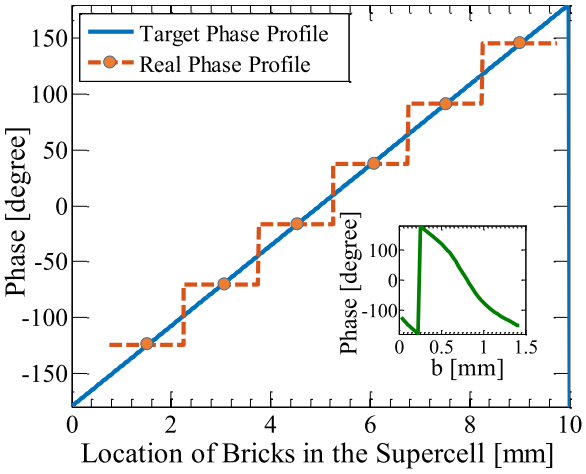

FIGURE 2. Target and real phase profile of the reflection for the deflection of a normally-incident plane wave at 30°. The inset shows the phase of the reflection from the unit cell of the metasurface as a function of *b*, the lateral dimension of silicon brick, varying in the range of 0.02-1.43 mm.

TABLE 1. The phase of the reflected wave from the unit cell of the metasurface by fixing a = 1 mm and the variation of b as the lateral dimension of the silicon brick.

Res	a [mm]	b [mm]	Phase [degree]
Res1	1	1.4	-120
Res2	1	1.09	-96
Res3	1	0.905	-42
Res4	1	0.78	+12
Res5	1	0.66	+66
Res6	1	0.5	+120

to the deflection of a normally-incident wave at an angle of 30°. As mentioned, there is no Ohmic loss in the resonators, and, due to the use of a metallic backplane, transmission is forbidden, resulting in virtually unitary reflectance.

To accurately study the performance of the VO_2-covered silicon resonators in terms of phase control, the effective index of the fundamental mode propagating in the z direction was calculated as a function of the lateral size b of the silicon brick (keeping the size a constant). Using periodic boundary conditions, a finite-element eigenmode solver (COMSOL) was adopted to solve the eigenmode problem in the xy-plane. Figure 3a illustrates how the electric field spatial distribution in the xy-plane varies as a function of the lateral size of the Si brick (b). The size-dependent enhancement of the electric field inside and around the Si resonator is associated with a size-dependent change in the effective mode index. The variation of the effective index produces, in turn, a variation of phase accumulated by the reflected wave, which can be calculated as $\phi = 2k_0 n_{eff} h_{Si}$. For this calculation, we assume that the eigenmode propagates for a round-trip (with total length $2h_{Si}$) inside the brick along the z direction. The phase as a function of b, retrieved from the effective index n_{eff} extracted by modal analysis is reported in Fig. 3b, and it shows good qualitative agreement with the full-wave simulations of Fig. 2.

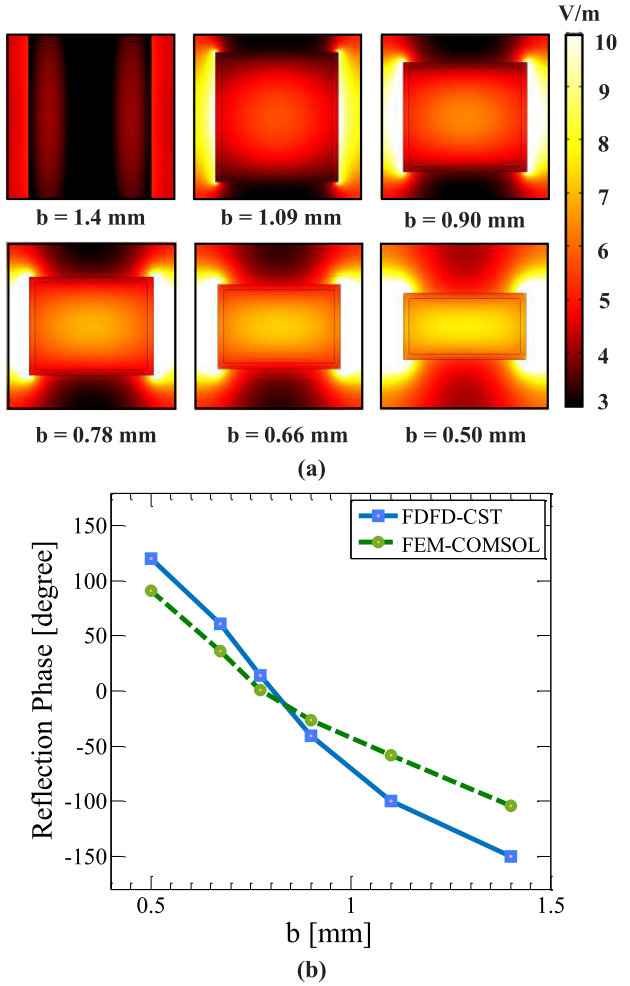

FIGURE 3. (a) Magnitude of electric field profile in the *xy*-plane as a function of the lateral dimension of the silicon brick. (b) The reflection phase as a function of *b*, the lateral dimension of the silicon brick, is calculated with two independent methods: full-wave simulations (FDFD method, blue curve); eigenmode solver (FEM method).

IV. PERFORMANCES OF THE RECONFIGURABLE METASURFACE

Next, we have simulated the supercell of the metasurface designed according to the procedure outlined in the previous section: it consists of six resonators, which are repeated periodically with a period of $6p$, as in Fig. 1. We assume an x-polarized plane wave impinging at normal incidence, and therefore we adopt periodic boundary conditions for the supercell, whose lateral size is $6p$ along the x-axis. This is a good approximation of a beam with a spot size significantly larger compared to the wavelength and to the supercell. The numerical results from the FDFD simulations in CST are presented in Fig.4 for VO_2 in the insulator state and Fig. 5 for VO_2 in the metallic state.

To investigate the detailed performance of the metasurface, we first calculated the reflectance in the millimeter wave bandwidth assuming VO_2 in the insulator state; the results are depicted in Fig. 4. The dominant contribution to reflection is in the wave directed at 30°, which shows an efficiency

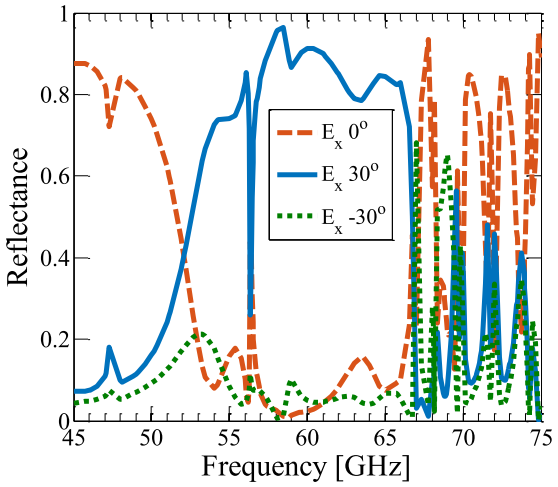

FIGURE 4. Reflectance from reconfigurable metasurface at temperatures lower than 68°C when VO_2 is in the insulator state.

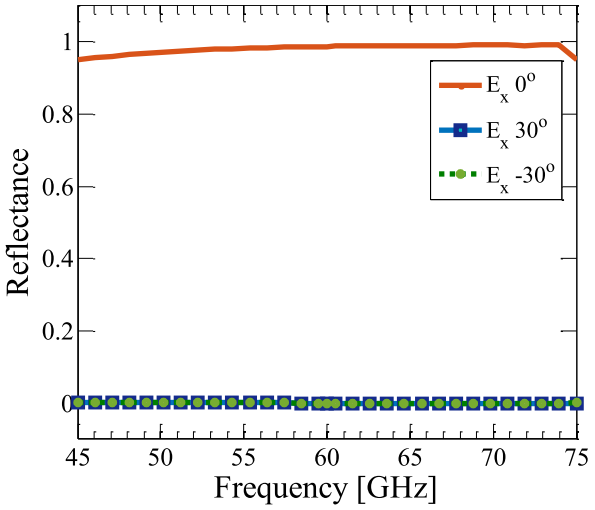

FIGURE 5. Reflectance from the reconfigurable metasurface at temperatures higher than 68°C when VO_2 is in the metallic state.

TABLE 2. Simulation parameters of the reconfigurable meta-reflectarray based on VO_2.

Ref.	Freq [GHz]	BW	Reflectance Average	Angle of Deflection
Insulator	60	57-66	0.86	30°
Metal	60	45-75	0.98	0°

TABLE 3. Features of the previous reconfigurable devices and the present device in frequency, bandwidth (BW), speed, efficiency η and functionality (Func).

Ref.	Freq [THz]	BW	η %	Func	Active Material	Conf[10]
[23]	0.7	-	-	MOD[1]	GST	IM[11]
[42]	1	-	30	DEF[2]	SDE[7]	II
[43]	307	3%	80	BS[3]	LC[8]	MIM
[44]	42.8	-	-	MOD	GPH[9]	MIM
[45]	0.3	-	-	DP[4]	CMOS	IM
[10]	0.037	7%	-	POL[5]	VO_2	MIM
[46]	0.01	10%	-	FIL[6]	VO_2	MIM
[47]	0.004	12%	-	FIL	VO_2	MIM
This work	0.06	15%	93	DEF	VO_2	MI

[1]Modulator, [2]Deflector, [3]Beam steering, [4]Digital programmable, [5]Polarizer, [6]Filter, [7]Schottky diode effect, [8]Liquid crystal, [9]Graphene, [10]Configuration, [11]Insulator-Metal.

of more than 80% in the range of frequencies 57-66 GHz, therefore providing a relative bandwidth of about 15% of anomalous reflection. Moreover, the *x*-polarized secondary lobes (i.e., other discrete diffraction orders), appearing at 0° and −30°, are lower than 20%; furthermore, the *y*-polarized reflectances are almost zero in any direction and, therefore, not reported in Fig. 4. In particular, the device efficiency at 60 GHz reaches 93%, which is remarkably higher in comparison to reconfigurable devices previously reported [42], [43].

In stark contrast, when the temperature of the structure increases over 68 °C, the VO_2 skin layer converts from insulators to metal, preventing an incident wave from reaching the silicon resonators. Thus, each part of the supercell creates the same phase profile causing the metasurface to reflect incident waves normally to the structure, in the specular direction. The wave reflectance has been calculated in the wide bandwidth between frequencies of 45GHz and 75GHz, as shown in Fig. 5. This graph indicates that the metasurface reflects millimeter waves in the specular direction with an efficiency close to 100%, while the other reflectance terms are almost zero. As shown in Figs. 4 and 5, when VO_2 switches from insulator to metal, the reflectance at 30° decreases to zero, causing the main power of reflection to be normal to the structure. Therefore, changing the temperature of the VO_2 layers provides a degree of tunability of deflection of millimeter waves. Table 2 shows the simulation parameters of the proposed reconfigurable metasurface based on VO_2 at both low and high temperatures.

For the realization of the proposed structure, a silicon layer with a thickness of 1.7 mm, equal to the thickness of silicon bricks, should be deposited on a copper layer with a thickness of 0.5 mm. Then, by performing lithography, the metasurface pattern with silicon resonators is transferred to the photoresist layer. After that, through etching, the pattern is created on the supercell of the metasurface. In the next step, a thin layer of VO_2 is covered the silicon bricks using a sputtering process. Temperature control can be achieved by passing an electric current through the back metal and exploiting the ohmic loss of copper. The critical problem in this process, which limits the tunability, is the fact that in a fabricated sample, VO_2 probably will not completely cover the vertical walls of the Si bricks. This can be mitigated by designing bricks with a conical shape.

A comparison of our structure with respect to other reconfigurable devices previously reported in the millimeter-wave range [10], [23], [42], [43], [44], [45], [46], [47] is summarized in Table 3, which highlights the strengths of the proposed metasurface configuration namely: large bandwidth, and high efficiency. The operational speed of this device is dependent on switching mechanisms for the VO_2 layer: the first mechanism is ultrafast (100 femtoseconds), which is

photo-induced, and that is only possible using high-intensity and short pulses as stimuli [48], and the second one is a slower one (nanosecond), purely thermal, which can be induced with electrical current, or heat [49].

V. CONCLUSION

In this paper, we presented a novel and simple architecture of a reconfigurable metasurface with engineered silicon bricks covered with a thin layer of VO_2 as a phase transition material, which provides wavefront engineering of an incident beam in the millimeter wave range. The device reflects the incident wave in an anomalous direction at temperatures at which VO_2 is an insulator. At temperatures above 68°C degrees, VO_2 switches reversibly to the metallic state, and the metasurface reflection occurs in the specular direction. Our numerical results indicate that thermal tuning of the metasurface is possible while maintaining an 80% efficiency over a relative bandwidth of 15% around 60 GHz, where it reaches an efficiency of 93%. The wideband operation in the millimeter-wave range, the high efficiency in anomalous reflection (low-temperature state of VO_2), and specular reflection (high-temperature state of VO_2) make the proposed device an appropriate candidate for high-resolution imaging, sensing, MIMO antennas for beam steering in high data rate and intelligent wireless communication systems, especially in beyond-5G and 6G cellular systems.

REFERENCES

[1] R. W. Heath, N. González-Prelcic, S. Rangan, W. Roh, and A. M. Sayeed, "An overview of signal processing techniques for millimeter wave MIMO systems," *IEEE J. Sel. Topics Signal Process.*, vol. 10, no. 3, pp. 436–453, Apr. 2016.

[2] A. Naqvi and S. Lim, "Review of recent phased arrays for millimeter-wave wireless communication," *Sensors*, vol. 18, no. 10, p. 3194, Sep. 2018.

[3] X. Wang, L. Kong, F. Kong, F. Qiu, M. Xia, S. Arnon, and G. Chen, "Millimeter wave communication: A comprehensive survey," *IEEE Commun. Surveys Tuts.*, vol. 20, no. 3, pp. 1616–1653, 3rd Quart., 2018.

[4] S. Tripathi, N. V. Sabu, A. K. Gupta, and H. S. Dhillon, "Millimeter-wave and terahertz spectrum for 6G wireless," in *6G Mobile Wireless Networks*. Cham: Springer, 2021, pp. 83–121.

[5] T. S. Rappaport, S. Sun, R. Mayzus, H. Zhao, Y. Azar, K. Wang, G. N. Wong, J. K. Schulz, M. Samimi, and F. Gutierrez, "Millimeter wave mobile communications for 5G cellular: It will work!" *IEEE Access*, vol. 1, pp. 335–349, 2013.

[6] W. Hong, Z. H. Jiang, C. Yu, D. Hou, H. Wang, C. Guo, Y. Hu, L. Kuai, Y. Yu, Z. Jiang, Z. Chen, J. Chen, Z. Yu, J. Zhai, N. Zhang, L. Tian, F. Wu, G. Yang, Z. Hao, and J. Y. Zhou, "The role of millimeter-wave technologies in 5G/6G wireless communications," *IEEE J. Microw.*, vol. 1, no. 1, pp. 101–122, Jan. 2021.

[7] C. Sturm and W. Wiesbeck, "Waveform design and signal processing aspects for fusion of wireless communications and radar sensing," *Proc. IEEE*, vol. 99, no. 7, pp. 1236–1259, Jul. 2011.

[8] L. Kong, M. K. Khan, F. Wu, G. Chen, and P. Zeng, "Millimeter-wave wireless communications for IoT-cloud supported autonomous vehicles: Overview, design, and challenges," *IEEE Commun. Mag.*, vol. 55, no. 1, pp. 62–68, Jan. 2017.

[9] A. Araghi, M. Khalily, P. Xiao, A. Kosari, H. Zarrabi, and R. Tafazolli, "Millimeter-wave MIMO balanced antipodal Vivaldi antenna design for autonomous cars," in *Proc. Int. Symp. Netw., Comput. Commun. (ISNCC)*, Jun. 2018, pp. 1–4.

[10] W. Yang, C. Zhou, Q. Xue, Q. Wen, and W. Che, "Millimeter-wave frequency-reconfigurable metasurface antenna based on vanadium dioxide films," *IEEE Trans. Antennas Propag.*, vol. 69, no. 8, pp. 4359–4369, Aug. 2021.

[11] M. R. M. Hashemi, S.-H. Yang, T. Wang, N. Sepúlveda, and M. Jarrahi, "Electronically-controlled beam-steering through vanadium dioxide metasurfaces," *Sci. Rep.*, vol. 6, no. 1, pp. 1–8, Oct. 2016.

[12] Q. Wang, X. G. Zhang, H. W. Tian, W. X. Jiang, D. Bao, H. L. Jiang, Z. J. Luo, L. T. Wu, and T. J. Cui, "Millimeter-wave digital coding metasurfaces based on nematic liquid crystals," *Adv. Theory Simulations*, vol. 2, no. 12, 2019, Art. no. 1900141.

[13] I. Ben Mabrouk, M. Al-Hasan, M. Nedil, T. A. Denidni, and A. Sebak, "A novel design of radiation pattern-reconfigurable antenna system for millimeter-wave 5G applications," *IEEE Trans. Antennas Propag.*, vol. 68, no. 4, pp. 2585–2592, Apr. 2020.

[14] Q. Guo and H. Wong, "Wideband and high-gain Fabry–Pérot cavity antenna with switched beams for millimeter-wave applications," *IEEE Trans. Antennas Propag.*, vol. 67, no. 7, pp. 4339–4347, Jul. 2019.

[15] P. Wang, J. Su, P. Ding, B. Mao, M. Ren, K. Xu, S. Tian, Y. Li, X. Tian, and J. Wang, "Graphene-metal based tunable radiative metasurface for information encryption and anticounterfeiting," *Diamond Rel. Mater.*, vol. 131, Jan. 2023, Art. no. 109548.

[16] S. K. Patel, J. Surve, V. Katkar, J. Parmar, F. A. Al-Zahrani, K. Ahmed, and F. M. Bui, "Encoding and tuning of THz metasurface-based refractive index sensor with behavior prediction using XGBoost regressor," *IEEE Access*, vol. 10, pp. 24797–24814, 2022.

[17] F. Bagheri and M. Soroosh, "Design and simulation of compact graphene-based plasmonic flip-flop using a resonant ring," *Diamond Rel. Mater.*, vol. 136, Jun. 2023, Art. no. 109904.

[18] X. Wang, X. He, J. Jiang, Y. Yao, and G. Lu, "Programmable manipulation of terahertz beams by hybrid graphene-metal coding metasurfaces," *Diamond Rel. Mater.*, vol. 129, Nov. 2022, Art. no. 109378.

[19] M. R. Eskandari, M. A. Shameli, and R. Safian, "Analysis of an electrically reconfigurable metasurface for manipulating polarization of near-infrared light," *J. Opt. Soc. Amer. B, Opt. Phys.*, vol. 39, no. 1, pp. 145–154, 2022.

[20] P. Thureja, G. K. Shirmanesh, K. T. Fountaine, R. Sokhoyan, M. Grajower, and H. A. Atwater, "Array-level inverse design of beam steering active metasurfaces," *ACS Nano*, vol. 14, no. 11, pp. 15042–15055, Nov. 2020.

[21] S. Xiao, T. Wang, T. Liu, C. Zhou, X. Jiang, and J. Zhang, "Active metamaterials and metadevices: A review," *J. Phys. D, Appl. Phys.*, vol. 53, no. 50, 2020, Art. no. 503002.

[22] X. Zhang, F. Fan, Y. Y. Ji, and S. J. Chang, "Temperature-dependent chirality of cholesteric liquid crystal for terahertz waves," *Opt. Lett.*, vol. 45, no. 18, pp. 4988–4991, 2020.

[23] P. Pitchappa, A. Kumar, S. Prakash, H. Jani, R. Medwal, M. Mishra, R. S. Rawat, T. Venkatesan, N. Wang, and R. Singh, "Volatile ultrafast switching at multilevel nonvolatile states of phase change material for active flexible terahertz metadevices," *Adv. Funct. Mater.*, vol. 31, no. 17, Apr. 2021, Art. no. 2100200.

[24] S. F. Jilani, M. O. Munoz, Q. H. Abbasi, and A. Alomainy, "Millimeter-wave liquid crystal polymer based conformal antenna array for 5G applications," *IEEE Antennas Wireless Propag. Lett.*, vol. 18, no. 1, pp. 84–88, Jan. 2019.

[25] L. Hu, X. Xu, X. Wen, M. Zhang, Y. Jing, X. Cheng, Y. Gu, T. Fan, and J. Xu, "Tunable organic metasurface based on 4-N, N-dimethylamino-4'-N'-methyl-stilbazolium tosylate (DAST) single crystal," *Opt. Commun.*, vol. 474, Nov. 2020, Art. no. 126114.

[26] S. Bulja, D. Mirshekar-Syahkal, R. James, S. E. Day, and F. A. Fernandez, "Measurement of dielectric properties of nematic liquid crystals at millimeter wavelength," *IEEE Trans. Microw. Theory Techn.*, vol. 58, no. 12, pp. 3493–3501, Dec. 2010.

[27] Z. Wang, Q. Chen, Y. Ma, T. Guo, C. Shuai, and Y. Fu, "Design of thermal-switchable absorbing metasurface based on vanadium dioxide," *IEEE Antennas Wireless Propag. Lett.*, vol. 21, no. 12, pp. 2302–2306, Dec. 2022.

[28] M. F. Jager, C. Ott, P. M. Kraus, C. J. Kaplan, W. Pouse, R. E. Marvel, R. F. Haglund, D. M. Neumark, and S. R. Leone, "Tracking the insulator-to-metal phase transition in VO_2 with few-femtosecond extreme UV transient absorption spectroscopy," *Proc. Nat. Acad. Sci. USA*, vol. 114, no. 36, pp. 9558–9563, Sep. 2017.

[29] W. Zeng, N. Chen, and W. Xie, "Research progress on the preparation methods for VO_2 nanoparticles and their application in smart windows," *CrystEngComm*, vol. 22, no. 5, pp. 851–869, 2020.

[30] J. Li, W. Yang, D. Chen, Q. Xue, Q. Wen, and W. Che, "Millimeter-wave frequency reconfigurable antenna using simple VO_2-based paired metasurface," *Int. J. RF Microw. Comput.-Aided Eng.*, vol. 32, no. 12, 2022, Art. no. e23454.

[31] H. Kim, N. Charipar, E. Breckenfeld, A. Rosenberg, and A. Piqué, "Active terahertz metamaterials based on the phase transition of VO_2 thin films," *Thin Solid Films*, vol. 596, pp. 45–50, Dec. 2015.
[32] X. Yang, X. Liu, S. Yu, L. Gan, J. Zhou, and Y. Zeng, "Permittivity of undoped silicon in the millimeter wave range," *Electronics*, vol. 8, no. 8, p. 886, Aug. 2019.
[33] J. Li, Y. Yang, J. Li, Y. Zhang, Z. Zhang, H. Zhao, F. Li, T. Tang, H. Dai, and J. Yao, "All-optical switchable vanadium dioxide integrated coding metasurfaces for wavefront and polarization manipulation of terahertz beams," *Adv. Theory Simulations*, vol. 3, no. 1, Jan. 2020, Art. no. 1900183.
[34] M. A. Shameli and L. Yousefi, "Absorption enhancement in thin-film solar cells using an integrated metasurface lens," *J. Opt. Soc. Amer. B*, vol. 35, no. 2, pp. 223–230, 2018.
[35] N. Yu, P. Genevet, M. A. Kats, F. Aieta, J.-P. Tetienne, F. Capasso, and Z. Gaburro, "Light propagation with phase discontinuities: Generalized laws of reflection and refraction," *Science*, vol. 334, no. 6054, pp. 333–337, Oct. 2011.
[36] S. M. Kamali, E. Arbabi, A. Arbabi, Y. Horie, and A. Faraon, "Highly tunable elastic dielectric metasurface lenses," *Laser Photon. Rev.*, vol. 10, no. 6, pp. 1002–1008, Nov. 2016.
[37] S. Tripathi, N. V. Sabu, A. K. Gupta, and H. S. Dhillon, "Millimeter-wave and terahertz spectrum for 6G wireless," in *6G Mobile Wireless Networks*. Cham, Switzerland: Springer, 2021, pp. 83–121.
[38] W. Kou, W. Shi, Y. Zhang, Z. Yang, T. Chen, J. Gu, X. Zhang, Q. Shi, S. Liang, F. Lan, H. Zeng, and Z. Yang, "Terahertz switchable focusing planar lens with a nanoscale vanadium dioxide integrated metasurface," *IEEE Trans. Terahertz Sci. Technol.*, vol. 12, no. 1, pp. 13–22, Jan. 2022.
[39] H. S. Sehmi, W. Langbein, and E. A. Muljarov, "Optimizing the drude-lorentz model for material permittivity: Method, program, and examples for gold, silver, and copper," *Phys. Rev. B, Condens. Matter*, vol. 95, no. 11, Mar. 2017, Art. no. 115444.
[40] S. Amador-Alvarado, J. M. Flores-Camacho, A. Solís-Zamudio, R. Castro-García, J. S. Pérez-Huerta, E. Antúnez-Cerón, J. Ortega-Gallegos, J. Madrigal-Melchor, V. Agarwal, and D. Ariza-Flores, "Temperature-dependent infrared ellipsometry of Mo-doped VO_2 thin films across the insulator to metal transition," *Sci. Rep.*, vol. 10, no. 1, p. 8555, May 2020.
[41] Y. V. Stebunov, D. I. Yakubovsky, D. Y. Fedyanin, A. V. Arsenin, and V. S. Volkov, "Superior sensitivity of copper-based plasmonic biosensors," *Langmuir*, vol. 34, no. 15, pp. 4681–4687, Apr. 2018.
[42] X. Su, C. Ouyang, N. Xu, W. Cao, X. Wei, G. Song, J. Gu, Z. Tian, J. F. O'Hara, J. Han, and W. Zhang, "Active metasurface terahertz deflector with phase discontinuities," *Opt. Exp.*, vol. 23, no. 21, pp. 27152–27158, 2015.
[43] S. Yin, D. Xiao, J. Liu, K. Li, H. He, S. Jiang, D. Luo, X. W. Sun, W. Ji, and Y. J. Liu, "Reconfigurable chiral metasurface absorbers based on liquid crystals," *IEEE Photon. J.*, vol. 10, no. 6, pp. 1–9, Dec. 2018.
[44] B. Zeng, Z. Huang, A. Singh, Y. Yao, A. K. Azad, A. D. Mohite, A. J. Taylor, D. R. Smith, and H.-T. Chen, "Hybrid graphene metasurfaces for high-speed mid-infrared light modulation and single-pixel imaging," *Light, Sci. Appl.*, vol. 7, no. 1, pp. 1–8, Aug. 2018.
[45] S. Venkatesh, X. Lu, H. Saeidi, and K. Sengupta, "A high-speed programmable and scalable terahertz holographic metasurface based on tiled CMOS chips," *Nature Electron.*, vol. 3, no. 12, pp. 785–793, Dec. 2020.
[46] D. Bouyge, A. Crunteanu, J. C. Orlianges, D. Passerieux, C. Champeaux, A. Catherinot, A. Velez, J. Bonache, F. Martin, and P. Blondy, "Reconfigurable bandpass filter based on split ring resonators and vanadium dioxide (VO2) microwave switches," in *Proc. Asia Pacific Microw. Conf.*, 2009, pp. 2332–2335.
[47] S. Yang, W. Li, M. Vaseem, and A. Shamim, "Additively manufactured dual-mode reconfigurable filter employing VO_2-based switches," *IEEE Trans. Compon., Packag., Manuf. Technol.*, vol. 10, no. 10, pp. 1738–1744, Oct. 2020.
[48] A. Pashkin, C. Kübler, H. Ehrke, R. Lopez, A. Halabica, R. F. Haglund, R. Huber, and A. Leitenstorfer, "Ultrafast insulator-metal phase transition in VO_2 studied by multiterahertz spectroscopy," *Phys. Rev. B, Condens. Matter*, vol. 83, no. 19, May 2011, Art. no. 195120.
[49] Y. Zhou, X. Chen, C. Ko, Z. Yang, C. Mouli, and S. Ramanathan, "Voltage-triggered ultrafast phase transition in vanadium dioxide switches," *IEEE Electron Device Lett.*, vol. 34, no. 2, pp. 220–222, Feb. 2013.

MOHAMMAD ALI SHAMELI was born in Isfahan, Iran, in 1993. He received the B.Sc. degree in electrical engineering from the Isfahan University of Technology, in 2015, and the M.Sc. and Ph.D. degrees in the fields and waves of electrical engineering from the University of Tehran, Tehran, Iran, in 2017 and 2021, respectively. He is currently a Postdoctoral Fellow with the University of Padova, Padua, Italy, where he is a member of the Photonics and Electromagnetics Group. His research interests include electromagnetics, photonics, and metamaterials.

ANTONIO-D CAPOBIANCO (Member, IEEE) received the B.Sc. degree in electronic engineering and the Ph.D. degree in electronic and telecommunication engineering from the University of Padova, Italy, in 1989 and 1994, respectively. He is currently an Associate Professor with the Department of Information Engineering, University of Padova. His current research interests include theory and numerical modeling in the fields of photonics, plasmonics, plasma, and microwave antennas.

LUCA SCHENATO (Member, IEEE) received the M.Sc. degree in telecommunication engineering and the Ph.D. degree in electronic and telecommunication engineering from the University of Padova, Padua, Italy, in 2003 and 2007, respectively. He is currently an Assistant Professor (RTDb) with the Department of Information Engineering, University of Padova. His current research interests include optical fiber sensors, optical fiber-based devices, metasurfaces, and intelligent reflective surfaces.

MARCO SANTAGIUSTINA (Member, IEEE) received the M.Sc. degree in electronic engineering and the Ph.D. degree in electronic and telecommunication engineering from the University of Padova, Padua, Italy, in 1992 and 1996, respectively. He is currently a Full Professor with the Department of Information Engineering, University of Padova. His current research interests include nonlinear optics, optical fibers, and electromagnetic field theory.

DOMENICO DE CEGLIA (Member, IEEE) received the "Laurea" and Ph.D. degrees in electrical engineering from Politecnico di Bari, Italy, in 2003 and 2007, respectively. He has been a Senior Research Associate with the National Research Council of the National Academies (USA). He is currently an Associate Professor of electromagnetic fields with the University of Brescia, Italy. His research interests include electromagnetics, optics and photonics, with an emphasis on plasmonics, nanophotonics, and nonlinear optics.

Open Access funding provided by 'Università degli Studi di Padova' within the CRUI CARE Agreement